Comparison between non-Markovian dynamics with and without rotating wave approximation*

Tang Ning(唐 宁), Xu Tian-Tian(徐甜甜), and Zeng Hao-Sheng(曾浩生)†

Key Laboratory of Low-Dimensional Quantum Structures and Quantum Control of Ministry of Education, and Department of Physics, Hunan Normal University, Changsha 410081, *China*

(Received 11 July 2012; revised manuscript received 20 August 2012)

In the limit of weak coupling between a system and its reservoir, we derive the time-convolutionless (TCL) non-Markovian master equation for a two-level system interacting with a zero-temperature structured environment with no rotating wave approximation (NRWA). By comparing the dynamics with RWA, we demonstrate the impact of RWA on the system dynamics, as well as the effects of non-Markovianity on the preservation of atomic coherence, squeezing, and entanglement.

Keywords: open quantum system, rotating wave approximation, non-Markovianity

PACS: 03.65.Ta, 03.65.Yz, 42.50.Lc **DOI:** 10.1088/1674-1056/22/3/030304

1. Introduction

Realistic quantum systems cannot avoid interactions with their environment, and thus the study of open quantum systems is very important. It is not only relevant to gaining a better understanding of quantum theory, but also fundamental for various modern applications of quantum mechanics, especially for quantum communication, quantum cryptography, and quantum computation.[1] The early studies of the dynamics of open quantum systems usually consisted of the application of an appropriate Born–Markov approximation. That is, neglecting all the memory effects, leading to a master equation that can be cast in the so-called Lindblad form.[2] Master equations in the Lindblad form can be characterized by the fact that the dynamics of the system satisfies both the semigroup property and the complete positivity, thus ensuring the preservation of the positivity of the density matrix during time evolution. We usually attribute the dynamical processes with these evolutional properties to the well-known Markovian ones.

However, people have recently found that many relevant physical systems, such as quantum optical systems,[3] quantum dots,[4] and superconductor systems,[5] cannot be simply described by Markovian dynamics. Similarly, quantum chemistry[6] and the excitation transfer in a biological system[7] also need to be treated as non-Markovian processes. Quantum non-Markovian processes can lead to distinctly different effects on the decoherence and disentanglement[8,9] of open systems compared to Markovian processes. These dynamical traits are important for enriching the basic theory of quantum mechanics, as well as for quantum information processing. Because of these distinct properties and extensive applications, more and more attention has been devoted to the study of the non-Markovian processes of open systems, including the measures of the non-Markovianity,[10–17] the positivity,[18,19] and some other dynamical properties[20–26] and the approaches[27,28] of non-Markovian processes. Experimentally, the simulation[29,30] of a non-Markovian environment has been realized.

The study of the dynamics of non-Markovian open quantum systems is typically very involved and often requires some approximations. Almost all the previous treatments are based on the rotating wave approximation (RWA), that is, neglecting the counter-rotating terms in the microscopic system–reservoir interaction Hamiltonian. However, the counter-rotating terms which are responsible for the virtual exchanges of energy between the system and the environment cannot always be neglected. Especially for the cases in which the transition of the system is large detuned from the dominant frequency of the environment or when the environment has a wide and flat spectrum, and then the RWA is invalid. The main motivation of this paper is thus to study the impact of the commonly-used RWA on the non-Markovian dynamics of the considered open quantum system. We also discuss the role of non-Markovianity on the preservation of atomic coherence, squeezing, and entanglement.

The article is organized as follows. In Section 2, we introduce the microscopic Hamiltonian model and derive the non-Markovian time-convolutionless (TCL) master equation for a two-level system weakly coupled to a vacuum reservoir with no RWA (NRWA). In Section 3, by choosing the Lorentzian spectrum as an exemplary example, we give the analytic expressions and the numerical simulation of the time-dependent decay rates. And we preliminarily demonstrate the effect of

*Project supported by the National Natural Science Foundation of China (Grant Nos. 11275064 and 11075050), the National Basic Research Program of China (Grant No. 2007CB925204), and the Construct Program of the National Key Discipline, China.

†Corresponding author. E-mail: hszeng@hunnu.edu.cn

© 2013 Chinese Physical Society and IOP Publishing Ltd

the counter-rotating wave terms on the dynamics of the open quantum system. In Section 4, we use the BLP measure to further analyze the impact of RWA on the non-Markovianity of the system dynamics. In Sections 5 and 6, we study, with NRWA, the non-Markovian dynamical behaviors of the atomic coherence, entropy squeezing, and entanglement. Finally, the conclusions are given in Section 7.

2. The microscopic model

Consider a two-level atom with Bohr frequency ω_0 interacting with a zero-temperature bosonic reservoir modeled by an infinite chain of quantum harmonic oscillators. The total Hamiltonian for this system in the Schrödinger picture is given by

$$H = \frac{1}{2}\omega_0\sigma_z + \sum_k \omega_k b_k^+ b_k + \sum_k g_k(\sigma_+ + \sigma_-)(b_k + b_k^+), \quad (1)$$

where σ_z and $\sigma_\pm$ are the Pauli and the inversion operators of the atom, and ω_k, b_k, and b_k^+ are the frequency, the annihilation and the creation operators for the k-th harmonic oscillator of the reservoir, respectively. The coupling strength g_k is assumed to be real for simplicity. The distinct feature of this Hamiltonian is the reservation of the counter-rotating wave terms $\sigma_+ b_k^+$ and $\sigma_- b_k$.

The TCL projection operator technique is most effective in dealing with the dynamics of open quantum systems. In the limit of weak coupling between the system and its environment, by expanding the TCL generator to the second order with respect to the coupling strength, the non-Markovian master equation describing the evolution of the reduced system in the interaction picture can be written as[3]

$$\frac{\mathrm{d}\rho(t)}{\mathrm{d}t} = -\mathrm{i}[H_{\mathrm{LS}}(t), \rho(t)] + D[\rho(t)] + D'[\rho(t)], \quad (2)$$

where

$$H_{\mathrm{LS}}(t) = S_+(t)\sigma_+\sigma_- + S_-(t)\sigma_-\sigma_+ \quad (3)$$

is the Lamb shift Hamiltonian, which describes a small shift in the energy of the eigenstate of the two-level atom. The dissipator $D[\rho(t)]$, which describes the secular motion of the system has the form

$$\begin{aligned} D[\rho(t)] = {} & \gamma_-(t)\left\{\sigma_-\rho(t)\sigma_+ - \frac{1}{2}\{\sigma_+\sigma_-, \rho(t)\}\right\} \\ & + \gamma_+(t)\left\{\sigma_+\rho(t)\sigma_- - \frac{1}{2}\{\sigma_-\sigma_+, \rho(t)\}\right\}, \end{aligned} \quad (4)$$

where the first term describes the dissipation of the atom to the vacuum environment with time-dependent decay rate $\gamma_-(t)$, and the second term denotes the heating of the atom in the vacuum environment with time-dependent heating rate $\gamma_+(t)$. This heating is related to the dissipation. For a ground-state atom in a zero-temperature environment, there would be no heating effect. The dissipator $D'[\rho(t)]$ represents the contribution of the so-called nonsecular terms, that is, terms oscillating rapidly with atomic transition frequency ω_0,

$$D'[\rho(t)] = [\alpha(t) + \mathrm{i}\beta(t)]\sigma_+\rho(t)\sigma_+ + \mathrm{h.c.}, \quad (5)$$

where h.c. denotes the Hermitian conjugation. In some cases, these nonsecular terms may be neglected via the so-called secular approximation. But in this paper we will include them into our consideration. The time-dependent coefficients in the above equations are

$$\gamma_\pm(t) = 2\int_0^t \mathrm{d}\tau \int \mathrm{d}\omega J(\omega)\cos[(\omega_0 \pm \omega)\tau], \quad (6)$$

$$S_\pm(t) = \pm\int_0^t \mathrm{d}\tau \int \mathrm{d}\omega J(\omega)\sin[(\omega_0 \mp \omega)\tau], \quad (7)$$

$$\alpha(t) = 2\int_0^t \mathrm{d}\tau \int \mathrm{d}\omega J(\omega)\cos[\omega(t-\tau)]\cos[\omega_0(t+\tau)], \quad (8)$$

$$\beta(t) = 2\int_0^t \mathrm{d}\tau \int \mathrm{d}\omega J(\omega)\cos[\omega(t-\tau)]\sin[\omega_0(t+\tau)], \quad (9)$$

where the spectral density function is defined as $J(\omega) = \sum_k g_k^2\delta(\omega - \omega_k)$.

Note that the dynamics of a two-level system embedded in a zero-temperature structured environment under the RWA has been already studied, and satisfies the master equation[3]

$$\begin{aligned} \frac{\mathrm{d}}{\mathrm{d}t}\rho(t) = {} & -\frac{\mathrm{i}}{2}S(t)[\sigma_+\sigma_-, \rho(t)] \\ & + \gamma(t)\left\{\sigma_-\rho(t)\sigma_+ - \frac{1}{2}\{\sigma_+\sigma_-, \rho(t)\}\right\}, \end{aligned} \quad (10)$$

with the time-dependent decay rate $\gamma(t)$ and Lamb shift $S(t)$ defined by

$$\gamma(t) = -2\mathrm{Re}\left[\frac{\dot{G(t)}}{G(t)}\right], \quad S(t) = -\mathrm{Im}\left[\frac{\dot{G(t)}}{G(t)}\right]. \quad (11)$$

This master equation has the following exact solution:[31]

$$\begin{aligned} \rho_{11}(t) &= |G(t)|^2\rho_{11}(0), \\ \rho_{00}(t) &= \rho_{00}(0) + [1 - |G(t)|^2]\rho_{11}(0), \\ \rho_{10}(t) &= G(t)\rho_{10}(0), \\ \rho_{01}(t) &= G^*(t)\rho_{01}(0), \end{aligned} \quad (12)$$

where $\rho_{ij} = \langle i|\rho|j\rangle$ with $|0\rangle$ and $|1\rangle$ are the ground and excited states of the two-level atom, respectively. The function $G(t)$ is defined as the solution of the integro–differential equation

$$\frac{\mathrm{d}}{\mathrm{d}t}G(t) = -\int_0^t \mathrm{d}t_1 f(t - t_1)G(t_1), \quad (13)$$

with the initial condition $G(0) = 1$. The kernel $f(t - t_1)$ denotes a two-point reservoir correlation function, which is the Fourier transformation of the spectral density $J(\omega)$

$$f(t - t_1) = \int \mathrm{d}\omega J(\omega)\exp[\mathrm{i}(\omega_0 - \omega)(t - t_1)]. \quad (14)$$

Comparing Eq. (2) with Eq. (10), we can see that both the decay rate $\gamma_-(t)$ and the Lamb shift $S_+(t)$ come from the rotating terms presented in the interaction Hamiltonian. In fact, by expanding the decay rate $\gamma(t)$ and the Lamb shift $S(t)$ to the second order with respect to the coupling strength, we obtain $\gamma_-(t)$ and $S_+(t)$.[3] However, the $\gamma_+(t)$ term in the dissipator $D[\rho(t)]$, as well as the nonsecular dissipator $D'[\rho(t)]$ and the Lamb shift $S_-(t)$, is purely from the contribution of the counter-rotating terms. In the following, we will show through further numerical simulations that these contributions from the counter-rotating terms can in some cases play an important role in the system dynamics, especially dynamical non-Markovianity.

3. Time-dependent decay rates

In order to clarify the impact of RWA on system dynamics, let us first discuss the contribution of the counter-rotating terms on the decay rates. We specify our study to a particular reservoir spectrum, the Lorentzian spectrum

$$J(\omega)=\frac{\gamma_0\lambda^2}{2\pi[(\omega_0-\omega-\Delta)^2+\lambda^2]}, \tag{15}$$

which describes the interaction of an atom with an imperfect cavity and is widely used in the literature. Here ω_0 denotes the transition frequency of the atom, $\Delta=\omega_0-\omega_c$ is the frequency detuning between the atom and the cavity mode, and λ is the width of the Lorentzian distribution, which is connected to the reservoir correlation time $\tau_R=\lambda^{-1}$. The parameter γ_0 can be regarded as the decay rate for the excited atom in the Markovian limit of the flat spectrum, which is related to the relaxation time $\tau_S=\gamma_0^{-1}$. For the Lorentzian spectrum, all the time-dependent coefficients in the master equation (2) can be calculated analytically and may be written as

$$\begin{aligned}\gamma_\pm(t) &= \frac{\gamma_0\lambda}{\lambda^2+\Delta_\pm^2}\{e^{-\lambda t}[\Delta_\pm\sin(\Delta_\pm t)\\ &\quad -\lambda\cos(\Delta_\pm t)]+\lambda\}, \qquad (16)\\ S_\pm(t) &= \pm\frac{\gamma_0\lambda}{2(\lambda^2+\Delta_\mp^2)}\{\Delta_\mp-e^{-\lambda t}[\lambda\sin(\Delta_\mp t)\\ &\quad +\Delta_\mp\cos(\Delta_\mp t)]\}, \qquad (17)\\ \alpha(t) &= \frac{\gamma_0\lambda}{2(\lambda^2+\Delta_+^2)}\{\lambda[\cos(2\omega_0 t)-e^{-\lambda t}\cos(\Delta t)]\\ &\quad +\Delta_+[\sin(2\omega_0 t)-e^{-\lambda t}\sin(\Delta t)]\}\\ &\quad +\frac{\gamma_0\lambda}{2(\lambda^2+\Delta^2)}\{\lambda[\cos(2\omega_0 t)-e^{-\lambda t}\cos(\Delta_+ t)]\\ &\quad +\Delta[\sin(2\omega_0 t)-e^{-\lambda t}\sin(\Delta_+ t)]\}, \qquad (18)\\ \beta(t) &= \frac{\gamma_0\lambda}{2(\lambda^2+\Delta_+^2)}\{\lambda[\sin(2\omega_0 t)-e^{-\lambda t}\sin(\Delta t)]\\ &\quad -\Delta_+[\cos(2\omega_0 t)-e^{-\lambda t}\cos(\Delta t)]\}\\ &\quad +\frac{\gamma_0\lambda}{2(\lambda^2+\Delta^2)}\{\lambda[\sin(2\omega_0 t)-e^{-\lambda t}\sin(\Delta_+ t)]\\ &\quad -\Delta[\cos(2\omega_0 t)-e^{-\lambda t}\cos(\Delta_+ t)]\}, \qquad (19)\end{aligned}$$

with $\Delta_-=\Delta=\omega_0-\omega_c$ and $\Delta_+=2\omega_0-\Delta=\omega_0+\omega_c$. Correspondingly, functions $G(t)$ and $\gamma(t)$ defined in Eqs. (11) and (12) become

$$G(t)=e^{-(\lambda-i\Delta)t/2}\left[\cosh\left(\frac{dt}{2}\right)+\frac{\lambda-i\Delta}{d}\sinh\left(\frac{dt}{2}\right)\right], \tag{20}$$

$$\gamma(t)=\mathrm{Re}\left[\frac{2\gamma_0\lambda\sinh(dt/2)}{d\cosh(dt/2)+(\lambda-i\Delta)\sinh(dt/2)}\right], \tag{21}$$

with $d=\sqrt{(\lambda-i\Delta)^2-2\gamma_0\lambda}$.

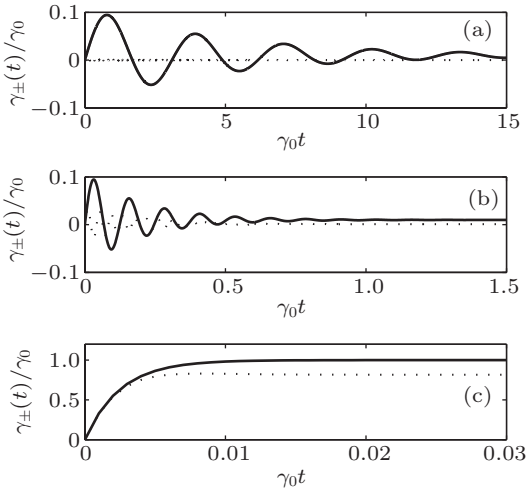


Fig. 1. The evolutions of the time-dependent decay rates. The solid and dotted lines correspond to the evolutions of γ_- and γ_+, respectively. We choose $\omega_0=100\gamma_0$, and $\lambda=0.2\gamma_0$, $\Delta=2\gamma_0$ in panel (a); $\lambda=5\gamma_0$, $\Delta=50\gamma_0$ in panel (b); $\lambda=400\gamma_0$, $\Delta=10\gamma_0$ in panel (c).

For different spectral widths and frequency detunings between the atom and the cavity mode, we plot the rescaled transition rates $\gamma_\pm(t)/\gamma_0$ as functions of dimensionless time $\gamma_0 t$ in Fig. 1, where we choose the atomic transition frequency to be $\omega_0=100\gamma_0$. For our purpose, we intentionally choose three special sets of parameters. This shows that for a narrow spectrum and a small detuning ($\lambda/\omega_0=0.2\%$, $\Delta/\omega_0=2\%$), $\gamma_-(t)$ plays the dominant role, while $\gamma_+(t)$ is almost zero. The results imply that for this set of parameters, the counter-rotating terms in Hamiltonian (1) have little effect on the system dynamics, and the commonly-used RWA is valid. However, for a wider spectrum and/or larger detuning, the results are different (see Figs. 1(b) and 1(c)), and γ_+ clearly cannot be neglected. Thus the counter-rotating terms in these cases are important, and the RWA is invalid. Of course for a very wide spectrum, we may expect that the system dynamics tend to be Markovian. The non-negativity of $\gamma_\pm(t)$ in Fig. 1(c) confirms this point. In addition, when λ is small, the correlation time of the environment is longer, thus γ_- in Fig. 1(a) oscillates to emerge with negative values in a relatively longer timescale. With the increasing λ, the correlation time becomes smaller and smaller, and the time for $\gamma_\pm$ to be negative shortens or even vanishes (Figs. 1(b) and 1(c)). Note that the visible negative

values of γ_+ in Fig. 1(b) demonstrate the contribution of the counter-rotating terms to the non-Markovianity of the system dynamics.

4. Non-Markovianity

Recently, researchers have been interested in the study of the non-Markovianity of open quantum systems. Several definitions or measures[10–13] of non-Markovian dynamics have been presented. Here, we employ the BLP measure[10] to quantify the non-Markovianity of the dynamics of the considered system. We will mainly highlight the impact of RWA on the non-Markovianity of the system's dynamics.

The BLP measure is based on the consideration in pure physics. Note that the Markovian processes always tend to continuously reduce the trace distance between any two states of a quantum system, thus an increase of the trace distance during any time interval implies the emergence of non-Markovianity. BLP links the changes of the trace distance to the flow of information between a system and its environment, and concludes that the back flow of information from the environment to the system is the key feature of non-Markovian dynamics. In quantum information science, the trace distance for quantum states ρ_1 and ρ_2 is defined as[1]

$$D(\rho_1,\rho_2)=\frac{1}{2}\mathrm{Tr}|\rho_1-\rho_2|, \tag{22}$$

with the trace norm defined as $|A|=\sqrt{A^\dagger A}$. For a given pair of initial states $\rho_{1,2}(0)$ of the system, the change in the dynamical trace distance can be described by its time derivative

$$\sigma(t,\rho_{1,2}(0))=\frac{\mathrm{d}}{\mathrm{d}t}D(\rho_1(t),\rho_2(t)), \tag{23}$$

where $\rho_{1,2}(t)$ are the dynamical states of the system corresponding to the initial states $\rho_{1,2}(0)$. For the Markovian processes, the monotonical reduction of the trace distance implies $\sigma(t,\rho_{1,2}(0))\leq 0$ for any initial states $\rho_{1,2}(0)$ at any time t. If a pair of initial states of the system exist such that for some evolutional time t the trace distance increases, that is, $\sigma(t,\rho_{1,2}(0))>0$, then the process must be non-Markovian. In the following we call the time intervals in which $\sigma(t)>0$ the information-backflow intervals (IBIs). BLP employs the sum of the areas of all the IBIs, i.e.,

$$\mathcal{N}=\max_{\rho_{1,2}(0)}\int_{\sigma>0}\sigma(t,\rho_{1,2}(0))\,\mathrm{d}t, \tag{24}$$

to quantify the non-Markovianity of a quantum process, where the maximum is taken over all pairs of initial states.

In order to calculate the BLP measure, we must solve the dynamics of the system. For this purpose, we rewrite the alternative Bloch equation of Eq. (2) as

$$\dot{b}_x=-\frac{1}{2}(\gamma_-+\gamma_+-2\alpha)b_x+(S_--S_+-\beta)b_y, \tag{25}$$

$$\dot{b}_y=-\frac{1}{2}(\gamma_-+\gamma_++2\alpha)b_y-(S_--S_+-\beta)b_x, \tag{26}$$

$$\dot{b}_z=-(\gamma_-+\gamma_+)b_z+\gamma_+-\gamma_-, \tag{27}$$

where the three components of the Bloch vector are defined as $b_j(t)=\mathrm{Tr}[\rho(t)\sigma_j]$ with $j=x,y,z$ and σ_j the Pauli operators. In terms of the Bloch vector, the trace distance of Eq. (22) may be expressed as

$$D(t)=\frac{1}{2}\sqrt{(\Delta b_x)^2+(\Delta b_y)^2+(\Delta b_z)^2}, \tag{28}$$

where $\Delta b_j=b_{1j}(t)-b_{2j}(t)$ are the differences between two Bloch components at time t. Correspondingly, the derivative of this trace distance becomes

$$\begin{aligned}\sigma=&-\frac{1}{8D(t)}[(\gamma_-+\gamma_+-2\alpha)(\Delta b_x)^2\\&+(\gamma_-+\gamma_++2\alpha)(\Delta b_y)^2\\&+4\beta(\Delta b_x)(\Delta b_y)+2(\gamma_-+\gamma_+)(\Delta b_z)^2],\end{aligned} \tag{29}$$

where we have used the Bloch Eqs. (25)–(27).

Note that in the RWA, by use of the exact solution (Eq. (12)), the derivative of the trace distance of Eq. (23) may be expressed as[32]

$$\sigma(t)=-\gamma(t)F(t). \tag{30}$$

The positive real function $F(t)$ is defined as

$$F(t)=\frac{a^2\mathrm{e}^{-\frac{3}{2}\Gamma(t)}+|b|^2\mathrm{e}^{-\frac{1}{2}\Gamma(t)}}{\sqrt{a^2\mathrm{e}^{-\Gamma(t)}+|b|^2}}, \tag{31}$$

with $\Gamma(t)=\int_0^t \mathrm{d}t'\gamma(t')$, and $a=\langle 1|\rho_1(0)|1\rangle-\langle 1|\rho_2(0)|1\rangle$, $b=\langle 1|\rho_1(0)|0\rangle-\langle 1|\rho_2(0)|0\rangle$ being the differences of the population and the coherence for the two given initial states, respectively.

In Fig. 2, we show the time evolution of the measure σ with the same parameters as those in Fig. 1, where the solid ones are plotted according to Eq. (29) and the dotted according to Eq. (30). We choose the pair of initial states to be $\rho_1(0)=|1\rangle\langle 1|$ and $\rho_2(0)=|0\rangle\langle 0|$, which can maximize the BLP measure.[10] As evidence, we only give the time intervals of $\sigma>0$, i.e., the IBIs. We can clearly see the effect of RWA on the non-Markovianity of the system's dynamics. In Fig. 2(a), both the distributions of the IBIs and the shapes of the two curves are similar, indicating that the counter-rotating terms have a lesser effect on the backflow of information in this case, which is in line with the RWA. The dip in each peak of the solid line in Fig. 2(b) is due to the negativity of $\gamma_+(t)$ at that time (see Fig. 1(b)), implying that γ_+ has the offset on the backflow of information. There is no IBI in Fig. 2(c), denoting that with this set of parameters, there is no backflow of information, or equivalently the dynamics is Markovian, which is in line with the non-negativity of $\gamma_\pm(t)$. All these results show

that the counter-rotating terms can affect the backflow of information. Note that the total area of IBIs in Fig. 2(a) is clearly larger than that in Fig. 2(b), implying that the former dynamics has larger degrees of non-Markovianity.

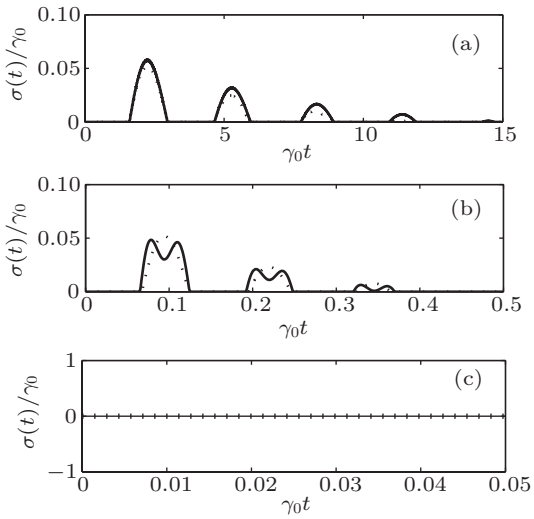


Fig. 2. The time evolution of $\sigma(t)$. The solid and dotted lines correspond to Eqs. (29) and (30), respectively, and the parameters in panels (a), (b), and (c) are set to be in accordance with those in Fig. 1.

5. Atomic coherence and entropy squeezing

Coherence and squeezing are two important quantities for describing atomic states. The coherence of a two-level atom may be described by the non-diagonal elements of its density matrix. As for the squeezing, here we employ the notion of information entropy squeezing. For a two-level atom with spin operators S_ν, $\nu = x, y, z$, the corresponding information entropies are defined as[33]

$$H(S_\nu) = -\sum_{i=1}^{2} p_i(S_\nu) \ln p_i(S_\nu), \tag{32}$$

where $p_i(S_\nu) = \langle \Psi_{\nu i}|\rho|\Psi_{\nu i}\rangle$ is the probability of the atom being in the eigenstate $|\Psi_{\nu i}\rangle$ of S_ν. A straightforward calculation for the two-level atom with density matrix ρ gives

$$\begin{aligned} H(S_x) &= -\left[\frac{1}{2}+\mathrm{Re}(\rho_{10})\right]\ln\left[\frac{1}{2}+\mathrm{Re}(\rho_{10})\right] \\ &\quad -\left[\frac{1}{2}-\mathrm{Re}(\rho_{10})\right]\ln\left[\frac{1}{2}-\mathrm{Re}(\rho_{10})\right], \qquad (33) \\ H(S_y) &= -\left[\frac{1}{2}+\mathrm{Im}(\rho_{10})\right]\ln\left[\frac{1}{2}+\mathrm{Im}(\rho_{10})\right] \\ &\quad -\left[\frac{1}{2}-\mathrm{Im}(\rho_{10})\right]\ln\left[\frac{1}{2}-\mathrm{Im}(\rho_{10})\right], \qquad (34) \\ H(S_z) &= -\rho_{11}\ln\rho_{11} - \rho_{00}\ln\rho_{00}. \qquad (35) \end{aligned}$$

Defining the information entropy squeezing factor

$$E(S_\nu) = \exp[H(S_\nu)] - \frac{2}{\sqrt{\exp[H(S_z)]}} \tag{36}$$

for $E(S_\nu) < 0$, we say that the fluctuation in component S_ν is squeezed in entropy.

As a typical example, here we consider the initial state of the atom to be

$$|\Phi\rangle = \frac{1}{\sqrt{2}}(|0\rangle + |1\rangle), \tag{37}$$

which has both optimal coherence and optimal entropy squeezing. Under RWA, the coherence, according to Eq. (12), is obtained as

$$|\rho_{10}(t)| = \frac{1}{2}|G(t)|. \tag{38}$$

And the entropy squeezing can be calculated by inserting Eq. (12) into Eq. (36). Alternatively, in the case of NRWA, we must first numerically evaluate the Bloch equation (25)–(27), obtain the initial state of Eq. (37), and then calculate the coherence and entropy squeezing.

In Fig. 3, we plot the time evolutions of the coherence with the same parameters as those in Fig. 1, where the solid and the dotted lines correspond to the cases of NRWA and RWA, respectively. We can clearly see that in general, the RWA leads the coherence to drop more slowly. In the case of non-Markovian evolutions (Figs. 3(a) and 3(b)), the coherence drops much slower compared with that in the Markovian case (Fig. 3(c)). This indicates that the non-Markovianity of the evolution process is beneficial to the preservation of atomic coherence. In addition, due to the stronger non-Markovianity for the evolution in Fig. 3(a), the coherence oscillates in time. While in Fig. 3(b), the non-Markovianity is too weak to oscillate visibly.

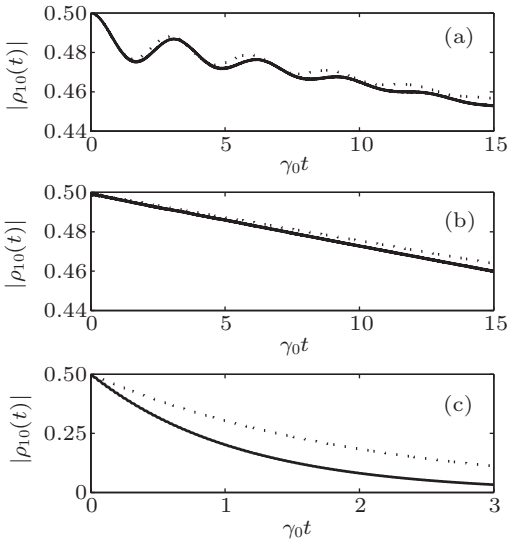


Fig. 3. The time evolution of coherence $|\rho_{10}(t)|$. The solid and dotted lines correspond to the NRWA and RWA cases, respectively, and the parameters in panels (a), (b), and (c) are set to be in accordance with those in Fig. 1.

In Figs. 4 and 5, we plot information entropy squeezing as a function of time with the same parameters as those in Fig. 1.

We can see that in Figs. 4(a) and 5(a), the solid and dotted lines are approximately in accordance, which once again shows that the RWA in this case is actually valid. While in panels (b) and (c) of these two figures, the visible corrections of the counter-rotating terms are observed, indicating the invalidation of the RWA. In addition, we find that for the non-Markovian evolutions, the information entropy can remain squeezed for a longer time (Figs. 4(a) and 4(b)), but for the Markovian evolution, the entropy squeezing vanishes very soon (Fig. 4(c)). Of course the quadrature components S_x and S_y cannot be squeezed simultaneously (see Fig. 5).

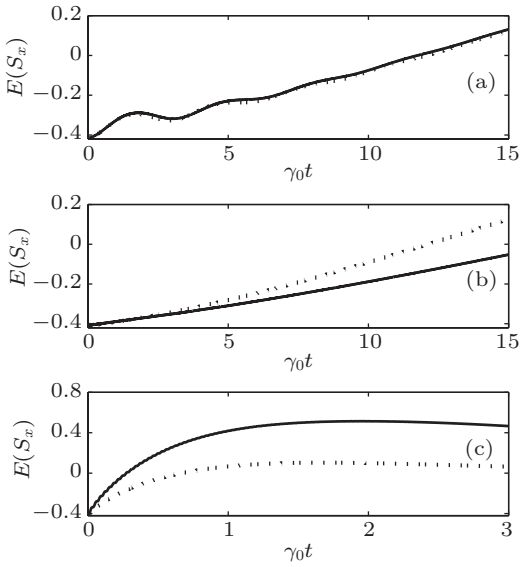


Fig. 4. The time evolution of entropy squeezing $E(S_x)$. The solid and dotted lines correspond to the NRWA and RWA cases, respectively, and the parameters in panels (a), (b), and (c) are set to be in accordance with those in Fig. 1.

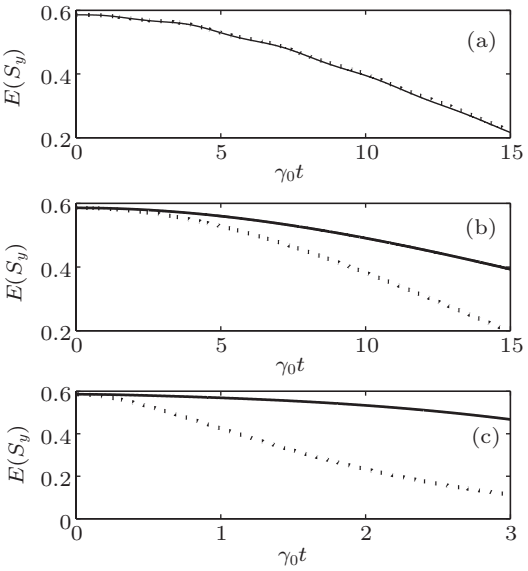


Fig. 5. The time evolution of entropy squeezing $E(S_y)$. The solid and dotted lines correspond to the NRWA and RWA cases, respectively, and the parameters in panels (a), (b), and (c) are set to be in accordance with those in Fig. 1.

6. Entanglement

At the end of this paper, we investigate the impact of RWA on entanglement. Consider two noninteracting qubits, A and B, each of which locally couples to a vacuum reservoir. According to the method presented in Ref. [34], the dynamics of the two-qubit system can be obtained simply from one of the individual qubits. Although the process applies to any form of the initial correlation state of the two-qubit system, for simplicity we only consider two types of Bell-like initial states

$$|\psi\rangle = \eta|00\rangle + \xi|11\rangle, \tag{39}$$

$$|\phi\rangle = \theta|01\rangle + \delta|10\rangle, \tag{40}$$

where η, ξ, θ, and δ are real and normalized as $\eta^2+\xi^2=1$ and $\theta^2+\delta^2=1$. Owing to the influence of the environment, the coherence of the open system will vanish asymptotically. Thus, the state of the system at any time t would be described by a density matrix. Under the product basis $\{|00\rangle,|01\rangle,|10\rangle,|11\rangle\} \equiv \{|1\rangle,|2\rangle,|3\rangle,|4\rangle\}$, the dynamical state of the two-qubit system can be written in the form $\rho(t) = [\rho_{ij}(t)]$ with $i,j=1,2,3,4$. Under RWA, the single qubit evolution is governed by Eq. (12). Thus the evolution of the two-qubit system can be calculated directly through the method presented in Ref. [34], which leads to the following nonzero elements:

$$\begin{aligned}
\rho_{11}(t) &= \eta^2 + (1-|G_{\rm A}|^2)(1-|G_{\rm B}|^2)\xi^2,\\
\rho_{22}(t) &= (1-|G_{\rm A}|^2)|G_{\rm B}|^2\xi^2,\\
\rho_{33}(t) &= |G_{\rm A}|^2(1-|G_{\rm B}|^2)\xi^2,\\
\rho_{44}(t) &= |G_{\rm A}|^2|G_{\rm B}|^2\xi^2,\\
\rho_{14}(t) &= G_{\rm A}^* G_{\rm B}^* \eta\xi,\\
\rho_{41}(t) &= G_{\rm A} G_{\rm B} \eta\xi
\end{aligned} \tag{41}$$

for initial state $|\psi\rangle$, and

$$\begin{aligned}
&\rho_{11}(t) = (1-|G_{\rm B}|^2)\theta^2 + (1-|G_{\rm A}|^2)\delta^2,\\
&\rho_{22}(t) = \theta^2|G_{\rm B}|^2, \quad \rho_{33}(t) = \delta^2|G_{\rm A}|^2,\\
&\rho_{23}(t) = \theta\delta G_{\rm A}^* G_{\rm B}, \quad \rho_{32}(t) = \theta\delta G_{\rm A} G_{\rm B}^*
\end{aligned} \tag{42}$$

for initial state $|\phi\rangle$. All the other matrix elements are zero. Here we use $G_{\rm A} \equiv G_{\rm A}(t)$ and $G_{\rm B} \equiv G_{\rm B}(t)$ to denote the $G(t)$ function for qubits A and B, respectively, which are determined by Eq. (13).

Using the results presented in the above section, we can study the evolution of quantum entanglement for given initial states. We use Wootters concurrence[35] as the measure of quantum entanglement. For a two-qubit system with density matrix ρ, the concurrence C is defined as

$$C = \max\{0, \lambda_1 - \lambda_2 - \lambda_3 - \lambda_4\}. \tag{43}$$

Here $\lambda_1 \geq \lambda_2 \geq \lambda_3 \geq \lambda_4$ are the square roots of the eigenvalues of matrix $R = \rho\widetilde{\rho}$, with $\widetilde{\rho} = \sigma_y^{(1)} \otimes \sigma_y^{(2)} \rho^* \sigma_y^{(1)} \otimes \sigma_y^{(2)}$, and the

sign $*$ standing for the complex conjugate. For the states given by Eqs. (41) and (42), the corresponding concurrences are

$$C_\psi(t) = \max\Big\{0, 2|G_A G_B \eta \xi| - 2\xi^2 |G_A G_B| \sqrt{(1-|G_A|^2)(1-|G_B|^2)}\Big\}, \quad (44)$$

$$C_\phi(t) = 2|\theta \delta G_A G_B|, \quad (45)$$

respectively. The notable characteristic is that the evolution of state $|\psi\rangle$ can have entanglement sudden death (ESD) when the condition $|\eta| - |\xi|\sqrt{(1-|G_A|^2)(1-|G_B|^2)} < 0$ is fulfilled.

The results of Eqs. (44) and (45) apply to any structured environment in principle. Here we assume that two identical qubits, A and B, are respectively plugged into the identical-structured but independent Lorentzian environments, such that $G_A = G_B = G(t)$, which is determined by Eq. (20). We also assume $\eta = \xi = \theta = \delta = 1/\sqrt{2}$, i.e., the maximally entangled Bell states. Note that for these Bell states, RWA predicts that there is no ESD in the evolution of entanglement.

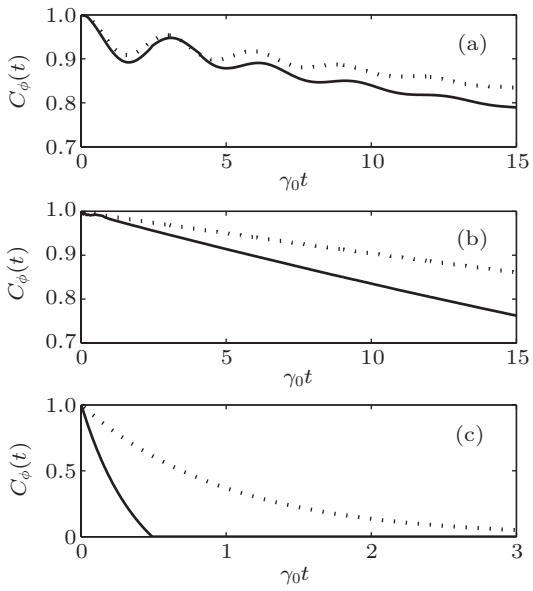


Fig. 6. The time evolution of concurrence for initial state $|\phi\rangle$. The solid and dotted lines correspond to the results of NRWA and RWA, respectively, and the parameters in panels (a), (b), and (c) are set to be in accordance with those in Fig. 1.

Without using RWA, the concurrence may be obtained by numerically evaluating Eqs. (25)–(27) along with Eq. (43) and using the method proposed in Ref. [34]. In Figs. 6 and 7, we plot the time evolutions of concurrence for maximally entangled states $|\phi\rangle = (|01\rangle + |10\rangle)/\sqrt{2}$ and $|\psi\rangle = (|00\rangle + |11\rangle)/\sqrt{2}$. We can see that on the whole, RWA slows down the dropping speeds of the concurrence. In Fig. 6(a), the dotted line is close to the solid one, showing the validity of RWA. But in Figs. 6(b) and 6(c), the deviation of the two lines becomes visibly large, indicating that RWA is no longer correct in these cases. In particular, in Fig. 6(c), the ESD that should occur in NRWA now vanishes, denoting that the RWA may obliterate the intrinsic properties of the dynamics of the open quantum system. In addition, the stronger non-Markovianity in Fig. 6(a) leads to the visible oscillations of concurrence. But in Fig. 6(b), the non-Markovianity is too weak to enable the concurrence to establish visible oscillations. Numerical simulations show that the non-Markovianity of the system dynamics is beneficial to the preservation of entanglement (comparing panels (a) and (b) with panel (c) in Figs. 6 and 7). The behavior shown in Fig. 7 is similar to that shown in Fig. 6. The only difference is that the results indicated by the two lines in Fig. 7(b) are not very large. This does not contradict the RWA, because the invalidity of RWA can but does not necessarily lead to a large deviation between the two results.

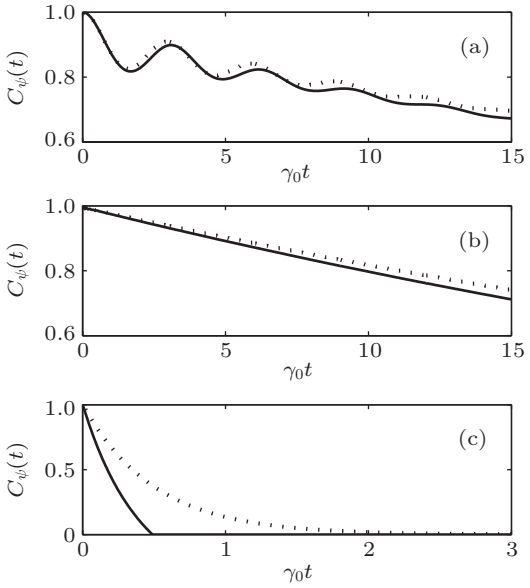


Fig. 7. The time evolution of concurrence for initial state $|\psi\rangle$. The solid and dotted lines correspond to the results of NRWA and RWA, respectively, and the parameters in panels (a), (b), and (c) are set to be in accordance with those in Fig. 1.

7. Conclusion

In conclusion, we studied the non-Markovian dynamical properties of a two-level system coupled to a zero-temperature structured environment under the NRWA. We derived the TCL master equation in the limit of weak coupling between the system and its environment. By comparing the NRWA result with that of RWA, we demonstrated the effect of RWA on the non-Markovianity, as well as on the coherence, squeezing, and entanglement of the system's dynamics. It is shown that for the case of large detuning between the system transition and the dominant frequency of the environment, or when the environment has a wide and flat spectrum, the RWA is invalid. The counter-rotating terms can provide remarkable corrections to the non-Markovianity of the system's dynamics. In general, the RWA slows down the vanishing speed of the coherence and the entanglement compared with the NRWA. In particular in some cases, the RWA may obliterate the ESD phenomenon

of the system. We also found that the non-Markovian effect is beneficial to the preservation of system coherence and entanglement, and helps the atom to be in a squeezed state for a much longer time.

References

[1] Nielsen M A and Chuang I L 2000 *Quantum Computation and Quantum Information* (Cambridge: Cambridge University Press)
[2] Lindblad G 1976 *Commun. Math. Phys.* **48** 119
[3] Breuer H P and Petruccione F 2007 *The Theory of Open Quantum Systems* (Oxford: Oxford University Press)
[4] Kubota Y and Nobusada K 2009 *J. Phys. Soc. Jpn.* **78** 114603
[5] Ji Y H and Hu J J 2010 *Chin. Phys. B* **19** 060304
[6] Shao J 2004 *J. Chem. Phys.* **120** 5053
[7] Chin A W, Datta A, Caruso F, Huelga S F and Plenio M B 2010 *New J. Phys.* **12** 065002
[8] Dijkstra A G and Tanimura Y 2010 *Phys. Rev. Lett.* **104** 250401
[9] Huang L Y and Fang M F 2010 *Chin. Phys. B* **19** 090318
[10] Breuer H P, Laine E M and Piilo J 2009 *Phys. Rev. Lett.* **103** 210401
[11] Rivas Á, Huelga S F and Plenio M B 2010 *Phys. Rev. Lett.* **105** 050403
[12] Usha Devi A R, Rajagopal A K and Sudha 2011 *Phys. Rev. A* **83** 022109
[13] Lu X M, Wang X G and Sun C P 2010 *Phys. Rev. A* **82** 042103
[14] Hou S C, Yi X X, Yu S X and Oh C H 2011 *Phys. Rev. A* **83** 062115
[15] Xu Z Y, Yang W L and Feng M 2010 *Phys. Rev. A* **81** 044105
[16] He Z, Zou J, Li L and Shao B 2011 *Phys. Rev. A* **83** 012108
[17] Zheng Y P, Tang N, Wang G Y and Zeng H S 2011 *Chin. Phys. B* **20** 110301
[18] Shabani A and Lidar D A 2009 *Phys. Rev. Lett.* **102** 100402
[19] Breuer H P and Vacchini B 2009 *Phys. Rev. E.* **79** 041147
[20] Haikka P and Maniscalco S 2010 *Phys. Rev. A* **81** 052103
[21] Chang K W and Law C K 2010 *Phys. Rev. A* **81** 052105
[22] Chruściński D, Kossakowski A and Pascazio S 2010 *Phys. Rev. A* **81** 032101
[23] Haikka P, Cresser J D and Maniscalco S 2011 *Phys. Rev. A* **83** 012112
[24] Ding B F, Wang X Y, Tang Y F, Mi X W and Zhao H P 2011 *Chin. Phys. B* **20** 060304
[25] Li C F, Wang H T, Yuan H Y, Ge R C and Guo G C 2011 *Chin. Phys. Lett.* **28** 120302
[26] Fang M F and Li Y L 2011 *Chin. Phys. B* **20** 100312
[27] Jing J and Yu T 2010 *Phys. Rev. Lett.* **105** 240403
[28] Wu C, Li Y, Zhu M and Guo Hong 2011 *Phys. Rev. A* **83** 052116
[29] Xu J S, Li C F, Gong M, Zou X B, Shi C H, Chen G and Guo G C 2010 *Phys. Rev. Lett.* **104** 100502
[30] Xu J S, Li C F, Zhang C J, Xu X Y, Zhang Y S and Guo G C 2010 *Phys. Rev. A* **82** 042328
[31] Laine E M, Piilo J and Breuer H P 2010 *Phys. Rev. A* **81** 062115
[32] Zeng H S, Tang N, Zheng Y P and Wang G Y 2011 *Phys. Rev. A* **84** 032118
[33] Fang M F, Zhou P and Swain S 2000 *J. Mod. Opt.* **47** 1043
[34] Bellomo B, Lo Franco R and Compagno G 2007 *Phys. Rev. Lett.* **99** 160502
[35] Wootters W K 1998 *Phys. Rev. Lett.* **80** 2245